A gastrolith protein serving a dual role in the formation of an amorphous mineral containing extracellular matrix

Assaf Shechter*, Lilah Glazer*, Shira Cheled*, Eyal Mor*, Simy Weil*, Amir Berman†‡§, Shmuel Bentov†‡, Eliahu D. Aflalo*‡, Isam Khalaila‡, and Amir Sagi*‡§

*Department of Life Sciences, ‡National Institute for Biotechnology in the Negev, †Department of Biotechnology Engineering, Ben Gurion University of the Negev, Beer-Sheva 84105, Israel

Edited by Joanna Aizenberg, Harvard University, Cambridge, MA, and accepted by the Editorial Board March 13, 2008 (received for review January 8, 2008)

Despite the proclamation of Lowenstam and Weiner that crustaceans are the "champions of mineral mobilization and deposition of the animal kingdom," relatively few proteins from the two main calcification sites in these animals, i.e., the exoskeleton and the transient calcium storage organs, have been identified, sequenced, and their roles elucidated. Here, a 65-kDa protein (GAP 65) from the gastrolith of the crayfish, *Cherax quadricarinatus*, is fully characterized and its function in the mineralization of amorphous calcium carbonate (ACC) of the extracellular matrix is demonstrated. GAP 65 is a negatively charged glycoprotein that possesses three predicted domains: a chitin-binding domain 2, a low-density lipoprotein receptor class A domain, and a polysaccharide deacetylase domain. Expression of *GAP 65* was localized to columnar epithelial cells of the gastrolith disk during premolt. *In vivo* administration of *GAP 65* dsRNA resulted in a significant reduction of *GAP 65* transcript levels in the gastrolith disk. Such gene silencing also caused dramatic structural and morphological deformities in the chitinous-ACC extracellular matrix structure. ACC deposited in these gastroliths appeared to be sparsely packed with large elongated cavities compared with the normal gastrolith, where ACC is densely compacted. ACC spherules deposited in these gastroliths are significantly larger than normal. GAP 65, moreover, inhibited calcium carbonate crystallization *in vitro* and stabilized synthetic ACC. Thus, GAP 65 is the first protein shown to have dual function, involved both in extracellular matrix formation and in mineral deposition during biomineralization.

amorphous calcium carbonate (ACC) | biomineralization | RNAi | Crustacea

Growth in crustaceans requires periodic shedding and replacement of the exoskeleton. In some crustaceans, molting occurs throughout the life cycle, whereas other species molt only until sexual maturity is reached (1). The crustacean exoskeleton, providing support, rigidity, and protection, comprises a chitinous organic matrix in which calcite or amorphous calcium carbonate (ACC) is deposited (2). In some crustacean species, such as the freshwater red claw crayfish *Cherax quadricarinatus*, calcium is mostly obtained from the diet but also from reabsorption from the exoskeleton before shedding and stored as stable ACC in transient calcium deposits (3). In crayfish, these deposits consist of a pair of disk-like structures known as gastroliths (4). Gastroliths, also found in other decapods (5), are extracellular constructs that form in a cavity between the gastrolith disk columnar epithelium and the cardiac stomach wall. The epithelium serves to transport hemolymph calcium into the gastrolith deposition site and participates in the synthesis of the gastrolith organic matrix (6).

The cyclic transport of calcium from the exoskeleton to temporary storage deposits and back is facilitated by the use of ACC, the most soluble form of calcium carbonate. In most crustaceans, exoskeleton calcium carbonate mainly exists in the stable crystalline form, i.e., calcite (5); however, in some species, it may also be deposited in the less stable amorphous form (7–9). It is thought that the latter represents the major form in most temporary calcium carbonate deposits, such as gastroliths in crayfish or sternal deposits in terrestrial Isopoda (9). We have previously reported that in *C. quadricarinatus*, ACC is the major form of calcium carbonate present, not only in the gastroliths, but also in the exoskeleton (10). Stabilization of otherwise unstable ACC likely requires the mediation of specialized macromolecules within the extracellular matrix.

The extracellular organic matrix in both the exoskeleton and transient storage organs is constructed from dense chitin–protein microfibrils (2, 5). Several matrix proteins of the crustacean exoskeleton related to the calcification process have been described in detail (5). Although the specific functions of these proteins remain poorly understood, they are suggested to assume roles in the inhibition/regulation of calcium carbonate precipitation and crystallization (7, 11–13).

The mechanism of calcium carbonate precipitation in transient storage organs of crustaceans is poorly understood, with only two transient storage organ proteins, namely orchestin and GAMP, having so far been identified. Orchestin is a calcium-binding protein isolated from the organic matrix of the calcium storage organ of the terrestrial crustacean, *Orchestia cavimana* (14). *In vitro* experiments revealed orchestin to interact with growing calcite crystals, with its calcium-binding capacities thought to depended on serine phosphorylation (11). Gastrolith matrix protein (GAMP), first isolated from the gastrolith of the crayfish, *Procambarus clarkii* (15), is believed to be a chitin-binding protein that inhibits calcium carbonate precipitation (16). Immunolocalization of GAMP revealed its presence at all stages of gastrolith growth and in certain layers of the exoskeleton (17).

Although orchestin and GAMP expressions are induced during premolt, detailed study of these calcification-related proteins is hampered by a lack of evidence regarding their *in vivo* roles. Molecular intervention techniques such as gene silencing may prove useful in remedying the situation. Thus far, the use of RNAi in crustaceans has been limited and aimed mostly at interfering with the expression of virus-related or neuropeptide-encoding genes (18, 19). Silencing of endogenous genes related to biomineralization has not been attempted until now.

In this study, we have identified and characterized a protein from the gastrolith matrix of the crayfish *C. quadricarinatus*. The dual role of this protein in gastrolith and extracellular matrix formation, together with its biomineralization function in sta-

Author contributions: A. Shechter, S.W., A.B., S.B., E.D.A., and A. Sagi designed research; A. Shechter, L.G., S.C., E.M., S.W., and S.B. performed research; A. Shechter and I.K. contributed new reagents/analytic tools; A. Shechter, A.B., S.B., E.D.A., and A. Sagi analyzed data; and A. Shechter, A.B., and A. Sagi wrote the paper.

The authors declare no conflict of interest.

This article is a PNAS Direct Submission. J.A. is a guest editor invited by the Editorial Board.

Data deposition: The sequence reported in this paper has been deposited in the GenBank Database (accession no. EU551670).

§To whom correspondence may be addressed. E-mail: sagia@bgu.ac.il or aberman@bgu.ac.il.

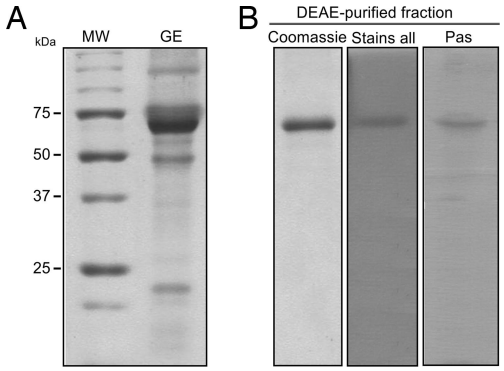

Fig. 1. Isolation of gastrolith proteins and purification of GAP 65. (*A*) Coomassie staining of the SDS/PAGE-generated protein profile of the gastrolith extract (GE) is shown on the right. Molecular mass markers (kDa) are shown on the left. (*B*) Pooled GAP 65-containing fractions collected at 1 M NaCl were purified by DEAE chromatography, separated by SDS/PAGE, and stained by Coomassie blue (left lane), ''Stains all'' (center lane), or Pas (right lane).

bilizing ACC, were tested using both *in vivo* gene silencing and *in vitro* precipitation of calcium carbonate.

Results

SDS/PAGE separation of EGTA-extracted gastrolith proteins revealed the presence of at least six distinct prominent proteins (Fig. 1*A*), with an ≈65-kDa species, termed GAP 65 (gastrolith protein 65) being most abundant. GAP 65-enriched HPLC fractions were separated by SDS/PAGE and detected with Coomassie brilliant blue, ''stains all'' (for negatively charged proteins), or periodic acid-Schiff's reagent (PAS) (for glycoproteins) (Fig. 1*B*), showing that GAP 65 is a negatively charged glycoprotein.

Fig. 2*A* presents the deduced amino acid sequence of GAP 65, including a predicted N-terminal signal sequence (amino acid 1–20). GAP 65 has a predicted pI of 5.01 and is not enriched in any specific amino acid. Approximately 4.6% of the total amino acids of GAP 65 represent possible phosphorylation sites, whereas only three predicted *N*-glycosylation sites and two putative *O*-glycosylation sites were detected. Bioinformatics analysis also suggests the presence of three known domains (Fig. 2*B*), i.e., chitin-binding domain 2 (ChtBD2, amino acids 29–102), a low-density lipoprotein receptor class A domain (LDLa, amino acids 122–159), and a polysaccharide deacetylase domain (amino acids 195–332). Of these, only the LDLa domain has predicted calcium-binding ability. The final 216 aa of the C-terminal do not offer indication of any known function.

The expression of *GAP 65* was tested in several target tissues by RT-PCR (Fig. 3*A*), with expression being detected in only the gastrolith epithelial disk and subepidermal tissue. Expression of *GAP 65 in situ* was localized to the columnar epithelial cells of the gastrolith disks of endocrinologically induced premolt but was not detected in untreated intermolt crayfish (Fig. 3*B*).

Transcript levels of crayfish injected with ecdysone (the steroid molting hormone) and silenced by *GAP 65* dsRNA were significantly lower than those found in the ecdysone- and dsRNA vehicle-injected crayfish (Fig. 4). In crayfish injected with ecdysone and *CqVg* dsRNA (a hepatopancreatic-specific gene found mostly in reproductive females that served as a control for sequence-specific silencing), *GAP 65* transcript levels were similar to those detected in the ecdysone- and dsRNA vehicle-injected group. In the control group, *GAP 65* transcript levels were higher than those found in the ecdysone- and *GAP 65* dsRNA-injected crayfish yet lower than what was detected in either ecdysone- and dsRNA vehicle-injected or ecdysone- and *CqVg* dsRNA-injected crayfish.

Morphological deformities of the gastrolith can be seen in crayfish injected with both *GAP 65* dsRNA and ecdysone (Fig. 5*A*), whereas, in crayfish injected with only ecdysone and the

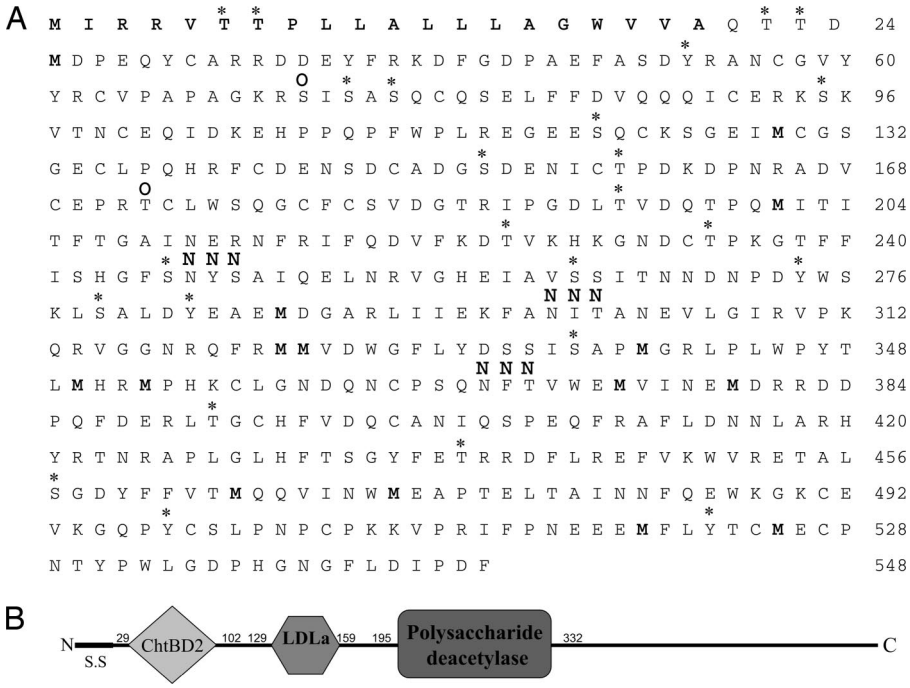

Fig. 2. Deduced amino acid sequence of GAP 65 and bioinformatics analysis of its sequence. (*A*) Deduced amino acid sequence of the GAP 65 ORF. Bold indicates predicted signal sequence, the asterisk indicates putative phosphorylation sites (NetPhos 2.0 server software), O indicates predicted *O*-glycosylation sites, and N indicates predicted *N*-glycosylation sites (YinOYang 1.2 software). (*B*) The complete GAP 65 sequence, showing the predicted signal sequence (S.S.) and the ChtBD2, LDLa, and polysaccharide deacetylase domains (SMART and Pfam software). Numbers indicate the amino acid range of each domain.

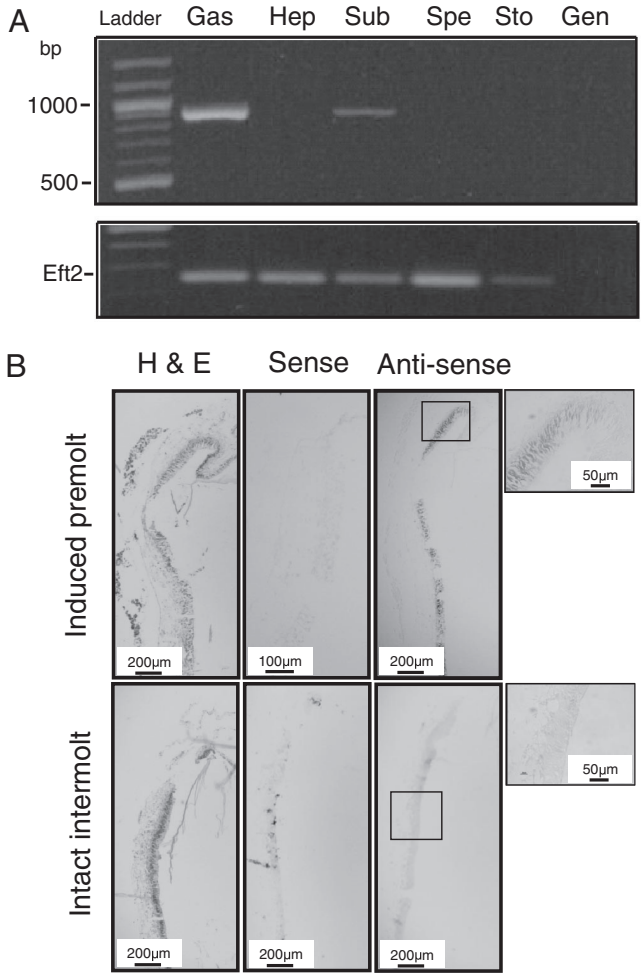

Fig. 3. Specific expression of *GAP 65* and its localization to the columnar epithelium of the gastrolith during induced premolt. (*A*) Detection of *GAP 65* expression during premolt by RT-PCR. RNA was extracted from gastrolith epithelial disk (Gas), hepatopancreas (Hep), subepidermal tissue (Sub), sperm duct (Spe), and stomach wall (Sto) tissues. Genomic control (Gen) was performed, and Elongation factor 2 (Eft2) was used to confirm RNA extraction. (*B*) Localization of *GAP 65* expression by *in situ* hybridization in induced premolt and intact intermolt males. (*Left*) H&E staining. (*Center*) Tissue probed with the negative control sense—*GAP 65* probe. (*Right*) Tissue probed with the GAP 65 antisense probe, with the far right image corresponding to an enlargement of a specific area (box in the antisense image). (Scale bar: 200 μm, except for in the induced premolt sense probe images, where it represents 100 μm and in the enlarged box, where it represents 50 μm.)

dsRNA vehicle, the gastrolith appeared normal, with no deformities. In the control group, the gastrolith appeared to be undeveloped. In crayfish injected with both *GAP 65* dsRNA and ecdysone, regions containing less dense mineral can be seen (arrows), although the gastrolith disk shape structure was retained. In the ecdysone- and dsRNA vehicle-injected crayfish, the gastroliths appeared normal with no effect on mineral densities (Fig. 5 *B* and *C*). Scanning electron microscope (SEM) images of gastroliths of crayfish injected with *GAP 65* dsRNA and ecdysone, furthermore, revealed severe ultrastructural abnormalities. The dense mineral and lamellar structure observed in normal gastroliths is replaced with a loosely packed, columnar mineralization structure, resembling hollow straws (Fig. 6 *A* and *B*). In these less dense gastroliths, spherule sizes ranged between 150 and 200 nm, whereas in the normal ACC deposited in the gastrolith, spherules ranged from 40 to 60 nm (Fig. 6*C*).

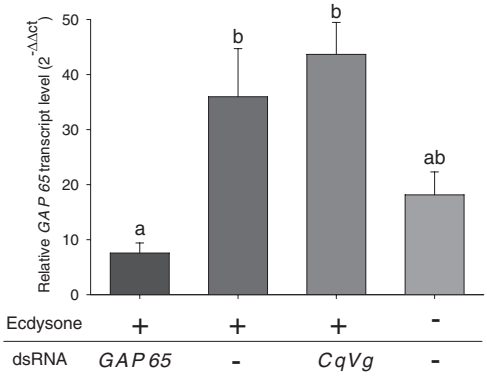

Fig. 4. Relative transcript levels of *GAP 65* in the gastrolith disk after *GAP 65* silencing. Real-time RT-PCR relative quantification of *GAP 65* transcript levels in the gastrolith disk of crayfish injected with (left to right): ecdysone and *GAP 65* dsRNA ($n = 7$), ecdysone and the dsRNA vehicle ($n = 6$), ecdysone and *C. quadricarinatus* vitellogenin (*CqVg*) dsRNA ($n = 3$), or the ecdysone and dsRNA vehicles ($n = 4$). Different letters above columns represent statistically significant differences ($P < 0.05 \pm$ SE).

Finally, to elucidate the role of GAP 65 in the biomineralization process, an *in vitro* calcium carbonate precipitation assay, testing the formation of stabilized synthetic ACC, was established. Precipitation in the presence of trypsin, serving as a control protein, resulted in the appearance of a crystalline precipitate of calcite crystals mixed with typical spherulitic vaterite aggregates, both ≈10 μm in size (Fig. 7*A*). On the other hand, precipitation in the presence of GAP 65 resulted in the deposition of mostly 40- to 60-nm ACC spherules, together with some calcite and vaterite (Fig. 7*B*). The ACC remained stable and did not crystallize for at least 2 months. Raman analysis confirmed the stabilized nature of the synthetic ACC generated in the presence of GAP 65 and its prolonged stability, as

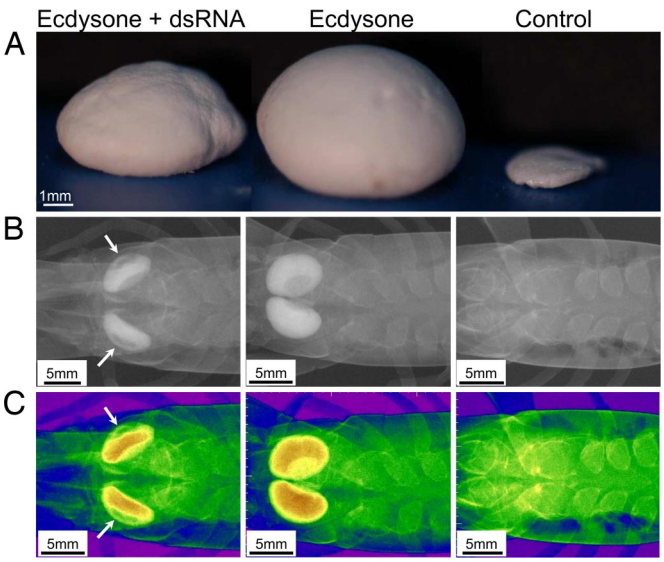

Fig. 5. Morphological deformities of the gastroliths after *GAP 65* silencing. Representative gastroliths, dissected from crayfish injected with ecdysone and *GAP 65* dsRNA (*Left*), ecdysone and the dsRNA vehicle (*Center*), or the ecdysone and dsRNA vehicles (*Right*). (*A*) Lateral view of the dissected gastroliths. (*B*) X-ray radiographs of the above gastrolith before dissection (dorsal view). (*C*) Mineral density assessment by color rendering of the x-ray images shown in *B*. The range of densities, from the highest to the lowest levels, is presented in yellow, green, blue, and purple. Arrows point to areas in the gastrolith where less mineral can be detected.

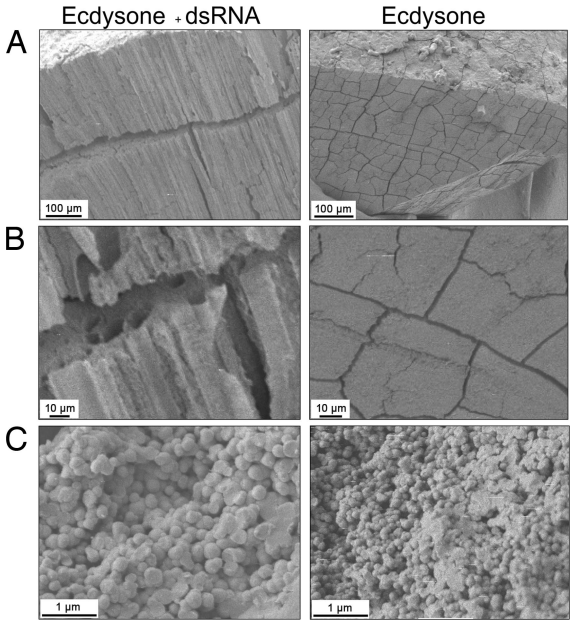

Fig. 6. SEM of gastroliths shows structural deformities after *GAP 65* silencing. Representative gastroliths dissected from crayfish injected with ecdysone and *GAP 65* dsRNA (*Left*) or the ecdysone and dsRNA vehicles (*Right*). (*A* and *B*) Cross-sections of the central part of the gastrolith, demonstrating the mineral and matrix arrangement. (Scale bars: 100 μm in *A* and 10 μm in *B*.) (*C*) Mineral nanospherule arrangement. (Scale bar: 1 μm.)

visualized by a distinct broad peak at 1,085 cm^{-1}, whereas in the presence of trypsin a sharp peak at 1,085 cm^{-1}, indicating the presence of calcite, is detected. The presence of occluded GAP 65 in the ACC formed by the *in vitro* precipitation assay was verified by purification of proteins extracted from the mineral fraction of the precipitate, including a predominant 65-kDa band, similar to that found within the GAP 65-enriched fractions (Fig. 7*C*).

Discussion

Currently, only two proteins from the biomineralized extracellular calcium carbonate deposits of crustaceans, namely orchestin (14) and GAMP (15), have been identified and characterized. In the present study, the protein-rich profile of the gastrolith of *C. quadricarinatus* was demonstrated, with the most abundant protein being GAP 65. In contrast to reports of other biomineralization-related proteins (13–15, 20), GAP 65 is not particularly enriched in any amino acid nor does it include any sequence motifs found in other crustacean calcification or cuticular proteins. It is of note that a 66-kDa PAS-positive, EDTA-soluble protein was identified in the exoskeleton of the blue crab, *Callinectes sapidus*. However, only the first 15 residues of this protein are known (21) and show no homology to GAP 65. A high degree of resemblance to GAP 65 is found in the *Drosophila melanogaster* proteins, vermiform and serpentine. These matrix proteins, found in the chitinous tracheal tubes, are responsible for limiting tracheal tube length by modulating the fibrillar structure of chitin (22, 23). Strikingly, GAP 65, vermiform and serpentine are almost 50% identical and all include the same three ChtBD2, LDLa, and polysaccharide deacetylase domains and possess a long stretch in the C-terminal region of unknown function. Mutation of these genes in *D. melanogaster* affected not only the trachea but also structural traits of the cuticle (22). The homology to vermiform and serpentine leads us to suggest that GAP 65 may serve a functional or regulatory role in the formation of the unique structure of the gastrolith chitinous matrix.

The Rebers–Riddiford chitin binding motif is, without doubt, the most widely spread motif in chitin-binding proteins found in the arthropod cuticle (24–26). However, no such domain is found in GAP 65. In turn, the less commonly found ChtBD2 motif, also known as the Peritrophin-A domain, was detected. To our knowledge, there are only rare reports of this domain in crustaceans, being found thus far solely in shrimp egg cortical crypts (27). The ChtBD2 domain was mostly reported in peritrophic matrix proteins of insects (28) and in some chitinases (29). At this point, one can only speculate why the most abundant protein in the gastrolith includes such a rare domain. Nevertheless, it was reported that two chitin-binding proteins, DE25 and DE29, isolated from the cuticle of the horseshoe crab, *Tachypleus tridentatus*, each contain six cysteine residues, similar to the cysteine-rich motif found in the ChtBD2 domain present in insect proteins (30). Although GAP 65 did present calcium-binding abilities, as observed in a radioactive calcium-binding assay (data not shown), the sequence of GAP 65 lacks any known calcium-binding motifs. These calcium-binding abilities may be, therefore, attributed to the LDLa domain, reported to afford calcium-binding to proteins in which it is found (31). Indeed, the exact role of the LDLa domain in a gastrolithic protein is not yet fully understood. The involvement of phosphorylated serines in calcium-binding crustaceans proteins has been claimed both in the case of CAP-1 (calcification-associated peptide), isolated from the exoskeleton of *Procambarus clarkii*, and in orchestin (32, 33) and may be involved in GAP 65 as well. Furthermore, although its primary function is the conversion of chitin into chitosan, the role of the polysaccharide deacetylase domain in GAP 65 function is not known.

Expression of *GAP 65* was detected in the gastrolith disk epithelium and in cuticle subepidermal tissue during gastrolith formation (premolt) but not in the gastrolith disk epithelium during intermolt, indicating the involvement of ecdysone in GAP 65 induction. The expression profile did, however, coincide with that reported for the only other protein isolated from the

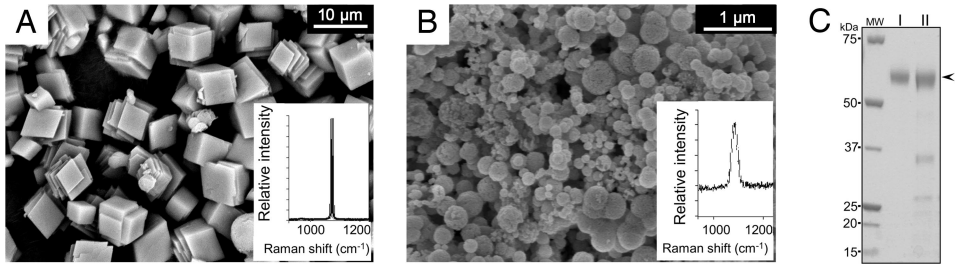

Fig. 7. *In vitro* precipitation of calcium carbonate in the presence of purified gastrolith proteins. (*A*) SEM image and Raman spectra of crystalline (calcite and vaterite) calcium carbonate precipitate in the presence of trypsin. (*B*) SEM image and Raman spectra of ACC precipitate in the presence of GAP 65-enriched fractions. (*C*) Coomassie-stained SDS/PAGE separation of GAP 65-enriched fractions (I) and protein extract from the synthetic ACC (II). MW, molecular mass markers. Arrowhead points to GAP 65.

gastrolith extracellular matrix, i.e., GAMP, which was detected in both tissues at the same molt stages (16).

The use of RNAi techniques to study biomineralization and the involvement of a "silenced" protein in the mineralization process has not previously been described. Before this study, successful injection of long dsRNA into a crustacean had been performed only in a small number of shrimp studies (19, 34). Here, sequence-specific reduction in *GAP 65* transcript levels was achieved by injection of long dsRNA, resulting in the formation of gastroliths with both morphological and structural deformities.

SEM images of the deformed gastroliths revealed a sparse, columnar-like arrangement, with elongated radial cavities including larger than normal ACC spherules. This abnormal appearance can be attributed to the effects of partial silencing of *GAP 65* production and secretion loci on the gastrolith epithelial membrane. GAP 65 deficiency is manifested both in the organization of the chitinous matrix and in the manner by which ACC spherules are accumulated.

Specific proteins or protein extracts from crustacean calcified tissues have been reported to act as *in vitro* inhibitors of calcium carbonate precipitation (16, 35) or as regulators of crystallization (11–13). It was suggested that CAP-1 might be involved in ACC stabilization in crayfish exoskeleton (7); however, no proof was provided. Indeed, this protein, together with orchestin and GAMP, are considerably different from GAP 65, with the latter lacking an acidic amino acids-rich sequence and possessing different characteristic domains. Protein extracts from the spicules of the sponge *Clathrina* and the ascidian *Pyura pachydermatina* have been reported (36, 37) to stabilize synthetic ACCs for up to 3 months. In this study, we demonstrate the capability of crustacean macromolecules to stabilize synthetic ACC. GAP 65 is a purified protein able to stabilize synthetic ACC that remains stable for up to 2 months. The manner by which GAP 65 stabilizes the ACC has yet to be elucidated.

The isolation of proteins from ACC-containing extracellular matrices, such as the crayfish gastrolith, holds potential for the fabrication of novel synthetic materials requiring stabilized synthetic amorphous minerals embedded into an extracellular chitinous framework. GAP 65 is a dual-function protein from the gastrolith, both interacting with the chitinous matrix and stabilizing ACC during the process of biomineralization.

Materials and Methods

Intermolt crayfish were endocrinologically induced through X-organ–sinus gland (XO–SG) complex removal to initiate premolt. The molt cycle was monitored by x-ray digital imaging to calculate the gastrolith molt mineralization index (MMI) (38). Gastroliths were dissected, cleaned, and ground to powder in liquid nitrogen. The powder was dissolved at a ratio of 1g per 20 ml of 0.02 M ammonium acetate (pH 7.0), 0.5 M EGTA on ice. The insoluble residue was separated by centrifugation (1,520 $\times$ *g* for 20 min at 4°C), and the supernatant was dialyzed against 0.2 M ammonium acetate (pH 7.0) at 4°C overnight. Dialysis was repeated twice, against 0.02 M and then 2 mM ammonium acetate. The samples were concentrated by using a Vivaspin 20 (MWCO 10,000; Vivascience) and transferred to a HiTrap desalting column (Amersham Biosciences).

Proteins were HPLC-separated by using fractogel EMD DEAE-650 S (Merck) column prewashed with 0.02 M ammonium acetate for 10 min, followed by a 70-min, 0–1 M NaCl gradient. The fractions collected at 1 M NaCl were separated by SDS/PAGE and stained with Coomassie blue, cationic carbocyanide stains-all dye (39) and PAS stain (40).

Reduction, alkylation, and trypsin digestion were carried out (41), followed by peptide extraction with 60% CH_3CN and 1% HCOOH. Dry peptide mixtures were dissolved with 0.1% HCOOH and subjected to nano-LC-MS analysis using a C_{18} nanocolumn connected in-line with a QTOF2 MS system (Micromass). The peptides were eluted in a linear gradient of 50% CH_3CN, 1% HCOOH. Analysis was performed by using the BioLynx package (Micromass), and database searches were performed with the Mascot package (Matrix Science) and BLAST. Partial sequencing of the peptides via MS–MS was used to construct the following degenerative primers: GAP 65 DGF (5′-ATGATGGTNGAYTGGGGNTTY-3′) and GAP 65 DGR (5′-AARTANCCIGANGTRAARTG-3′), used in a RT-PCR with gastrolith epithelial disk RNA. The entire *GAP 65* sequence was obtained through rapid amplification of 5′ and 3′ cDNA ends (RACE; Clontech SMART RACE; BD Biosciences).

Tissue-specific expression was assessed by RT-PCR with the following primers: 65–900bpF (5′-GGGTGGTCGCCCAGACCACAGAC ATGGA-3′) and 65–900bpR (5′-ACCAACTCGCTGCTTGGGGACGCGGATT-3′).

Histological preparation and *in situ* hybridization were performed (42) by using antisense and sense *GAP 65* cDNA riboprobes.

For dsRNA synthesis, a *GAP 65* amplicon was generated by using the primers Fsi-GAP65 (5′-CATCAGTGCCTCCCAGTGCCAGAGTG-3′) and Rsi-GAP65 (5′-TCGTTGCCCTTGTGCTTGACGGTGTCC-3′) and cloned into the pGEM-Teasy vector (Promega). This plasmid served as template for two PCRs, the first using the primers, Fsi–GAP65 and RsiOH–GAP65 (5′-TAATACGACTCACTATAGGGATCGTTGCCCTTGTGCTTGACG GTGTCC-3′) and the second using FsiOH–GAP65 (5′-TAATACGACTCACTA TAGGGACATCAGTG CCTCCCAGTGCCAGAGTG-3′) and Rsi–GAP65. The entire procedure was repeated, by using *CqVg* (42), with the following primers: CqVg SiF (5′-ACTTCCCTCTCCTACTGTTG-3′), CqVg SiR (5′-TCTTGCAGCTGTTCCAGTAG-3′), CqVg Si OHF (5′-TAATACGACTCACT ATAGGGACTTCCCTCTCCTACTGTTG-3′) and CqVg Si OHR (5′-TAATACGA CTCACTATAGGGTCTTGCAGCTGTTCCAGTAG-3′). The amplicons then served as templates for single-strand RNA synthesis (MEGAscript; Ambion). The single-stand RNA was purified by using phenol–chloroform and resuspended in double distilled water, incubated at 65°C for 5 min with its complementary strand at room temperature for 5 min and stored at −70°C.

dsRNA was injected at a fixed dose of 50 μg, whereas ecdysone was injected to a final concentration of 1 ng/μl (38). In this study, the term ecdysone refers to the use of α-ecdysone (also termed ecdysone). We found that the use of α-ecdysone required less frequent injections to achieve gastrolith formation than are required when using 20E (data not shown). Control animals were injected with comparable amounts of 10% ethanol in saline. Twenty intermolt males (MMI = 0) with an average weight of 13.5 $\pm$ 1.4 g (SE) were used. Injections of dsRNA into the fifth walking leg sinus were performed on days 1, 3, 5, and 7, whereas ecdysone was injected daily until day 9. At the end of the experiment, all crayfish were anesthetized in ice-cold water and dissected.

RNA was extracted from the gastrolith disk as above, and real-time RT-PCR to evaluate *GAP 65* transcript levels (38) was performed by using the primers GAP 65 QF1-F (5′-AGATCG CCGTCAGTTCCATC-3′) and GAP 65QR1-R (5′-AATGAGA CGAGCACCATC CAT-3′), and 18S rRNA served as the normalizing agent (38). Values are expressed as mean $\pm$ SE. One-way ANOVA was performed by using P values <0.05.

SEM (FEI quanta 200) was performed after gold sputtering of gastrolith fractures at an acceleration voltage of 10–15 kV.

In vitro precipitation of gastrolith proteins (10 μg/ml) was achieved by using a 10 mM $CaCl_2$ solution containing 10 mM Na_2CO_3. After centrifugation (1,520 $\times$ *g* for 5 min at 4°C), the precipitate was spread over a glass slide, instantly air dried, and observed with a light microscope. Raman measurements were made by using a 600-grooves mm^{-1} grating and a confocal microscope with a 100-μm aperture, giving a resolution of 4–8 cm^{-1}. Spectra were scanned for 60 sec in the 200- to 1,400-cm^{-1} range (Jobin–Yvon LabRam HR 800 microRaman). The ACC precipitate was dissolved with 10 ml of 0.5 M EGTA, 0.02 M ammonium acetate (pH 7.0) and dialyzed. Extracted protein and GAP 65-enriched fractions were separated by SDS/PAGE.

ACKNOWLEDGMENTS. Technical assistance by Mr. Liron Friedman and Mr. Oren Levi is highly appreciated. This work was supported by Israel Science Foundation Grant 1080/05 and a grant from Amorphical, Ltd.

1. Hartnoll RG (1982) in *The Biology of Crustacea*, ed Bliss DE (Academic, New York), Vol 2, pp 111–197.
2. Lowenstam HA, Weiner S (1989) *On Biomineralization* (Oxford Univ Press, New York).
3. Travis DF, Friberg U (1963) The deposition of skeletal structures in the crustacea. IV. Microradiographic studies of the gastrolith of the crayfish *Orconectes virilis hagen. J Ultrastruct Res* 8:48–65.
4. Travis DF (1960) The deposition of skeletal structures in the Crustacea. 1. The histology of the gastrolith skeletal tissue complex and the gastrolith in the crayfish, *Orconectes (Cambarus) verilis* Hagen-Decapoda. *Biol Bull* 118:137–149.
5. Luquet G, Marin F (2004) Biomineralisations in crustaceans: Storage strategies. *C R Palevol* 3:515–534.
6. Ueno M (1980) Calcium-transport in crayfish gastrolith disk—morphology of gastrolith disk and ultrahistochemical demonstration of calcium. *J Exp Zool* 213:161–171.
7. Sugawara A, *et al.* (2006) Self-organization of oriented calcium carbonate/polymer composites: Effects of a matrix peptide isolated from the exoskeleton of a crayfish. *Angew Chem Int Ed* 45:2876–2879.
8. Greenaway P (1985) Calcium balance and molting in the crustacea. *Biol Rev Camb Philos Soc* 60:425–454.

9. Addadi L, Raz S, Weiner S (2003) Taking advantage of disorder: Amorphous calcium carbonate and its roles in biomineralization. *Adv Mater* 15:959–970.
10. Shechter A, *et al.* (2008) Reciprocal changes in calcification of the gastrolith and cuticle during the molt cycle of the red claw crayfish *Cherax quadricarinatus. Biol Bull (Woods Hole)* 214:122–134.
11. Hecker A, *et al.* (2004) Orchestin, a calcium-binding phosphoprotein, is a matrix component of two successive transitory calcified biomineralizations cyclically elaborated by a terrestrial crustacean. *J Struct Biol* 146:310–324.
12. Coblentz FE, Shafer TH, Roer RD (1998) Cuticular proteins from the blue crab alter *in vitro* calcium carbonate mineralization. *Comp Biochem Physiol* 121:349–360.
13. Endo H, Takagi Y, Ozaki N, Kogure T, Watanabe T (2004) A crustacean Ca^{2+}-binding protein with a glutamate-rich sequence promotes $CaCO_3$ crystallization. *Biochem J* 384:159–167.
14. Testeniere O, *et al.* (2002) Characterization and spatiotemporal expression of orchestin, a gene encoding an ecdysone-inducible protein from a crustacean organic matrix. *Biochem J* 361:327–335.
15. Ishii K, Yanagisawa T, Nagasawa H (1996) Characterization of a matrix protein in the gastroliths of the crayfish *Procambarus clarkii. Biosci Biotechnol Biochem* 60:1479–1482.
16. Tsutsui N, Ishii K, Takagi Y, Watanabe T, Nagasawa H (1999) Cloning and expression of a cDNA encoding an insoluble matrix protein in the gastroliths of a crayfish, *Procambarus clarkii. Zool Sci* 16:619–628.
17. Takagi Y, Ishii K, Ozaki N, Nagasawa H (2000) Immunolocalization of gastrolith matrix protein (GAMP) in the gastroliths and exoskeleton of crayfish, *Procambarus clarkii. Zool Sci* 17:179–184.
18. Yodmuang S, Tirasophon W, Roshorm Y, Chinnirunvong W, Panyim S (2006) YHV-protease dsRNA inhibits YHV replication in *Penaeus monodon* and prevents mortality. *Biochem Biophys Res Commun* 341:351–356.
19. Tiu SH, Chan SM (2007) The use of recombinant protein and RNA interference approaches to study the reproductive functions of a gonad-stimulating hormone from the shrimp *Metapenaeus ensis. FEBS J* 274:4385–4395.
20. Inoue H, Ozaki N, Nagasawa H (2001) Purification and structural determination of a phosphorylated peptide with anti-calcification and chitin-binding activities in the exoskeleton of the crayfish, *Procambarus clarkii. Biosci Biotechnol Biochem* 65:1840–1848.
21. Tweedie EP, Coblentz FE, Shafer TH (2004) Purification of a soluble glycoprotein from the uncalcified ecdysial cuticle of the blue crab *Callinectes sapidus* and its possible role in initial mineralization. *J Exp Biol* 207:2589–2598.
22. Luschnig S, Batz T, Armbruster K, Krasnow MA (2006) Serpentine and Vermiform encode matrix proteins with chitin binding and deacetylation domains that limit tracheal tube length in *Drosophila. Curr Biol* 16:186–194.
23. Wang S, *et al.* (2006) Septate-junction-dependent luminal deposition of chitin deacetylases restricts tube elongation in the *Drosophila* trachea. *Curr Biol* 16:180–185.
24. Andersen SO (1998) Characterization of proteins from arthrodial membranes of the lobster, *Homarus americanus. Comp Biochem Physiol* 121:375–383.
25. Faircloth LM, Shafer TH (2007) Differential expression of eight transcripts and their roles in the cuticle of the blue crab, *Callinectes sapidus. Comp Biochem Physiol* 146:370–383.
26. Andersen SO (2000) Studies on proteins in post-ecdysial nymphal cuticle of locust, *Locusta migratoria*, and cockroach, *Blaberus craniifer. Insect Biochem Mol Biol* 30:569–577.
27. Du XJ, *et al.* (2006) Identification and molecular characterization of a peritrophin-like protein from fleshy prawn (*Fenneropenaeus chinensis*). *Mol Immunol* 43:1633–1644.
28. Elvin CM, *et al.* (1996) Characterization of a major peritrophic membrane protein, peritrophin-44, from the larvae of *Lucilia cuprina* cDNA and deduced amino acid sequences. *J Biol Chem* 271:8925–8935.
29. Shen Z, Jacobs-Lorena M (1998) A type I peritrophic matrix protein from the malaria vector *Anopheles gambiae* binds to chitin. Cloning, expression, and characterization. *J Biol Chem* 273:17665–17670.
30. Iijima M, *et al.* (2005) Comprehensive sequence analysis of horseshoe crab cuticular proteins and their involvement in transglutaminase-dependent cross-linking. *FEBS J* 272:4774–4786.
31. Rodenburg KW, Van der Horst DJ (2005) Lipoprotein-mediated lipid transport in insects: analogy to the mammalian lipid carrier system and novel concepts for the functioning of LDL receptor family members. *Biochim Biophys Acta* 1736:10–29.
32. Hecker A, Testeniere O, Marin F, Luquet G (2003) Phosphorylation of serine residues is fundamental for the calcium-binding ability of orchestin, a soluble matrix protein from crustacean calcium storage structures. *FEBS Lett* 535:49–54.
33. Inoue H, Ohira T, Ozaki N, Nagasawa H (2003) Cloning and expression of a cDNA encoding a matrix peptide associated with calcification in the exoskeleton of the crayfish. *Comp Biochem Physiol* 136:755–765.
34. Robalino J, *et al.* (2007) Double-stranded RNA and antiviral immunity in marine shrimp: Inducible host mechanisms and evidence for the evolution of viral counter-responses. *Dev Comp Immunol* 31:539–547.
35. Inoue H, Ohira T, Ozaki N, Nagasawa H (2004) A novel calcium-binding peptide from the cuticle of the crayfish, *Procambarus clarkii. Biochem Biophys Res Commun* 318:649–654.
36. Aizenberg J, Lambert G, Addadi L, Weiner S (1996) Stabilization of amorphous calcium carbonate by specialized macromolecules in biological and synthetic precipitates. *Adv Mater* 8:222–226.
37. Aizenberg J, Lambert G, Weiner S, Addadi L (2002) Factors involved in the formation of amorphous and crystalline calcium carbonate: A study of an ascidian skeleton. *J Am Chem Soc* 124:32–39.
38. Shechter A, *et al.* (2007) Search for hepatopancreatic ecdysteroid-responsive genes during the crayfish molt cycle: from a single gene to multigenicity. *J Exp Biol* 210:3525–3537.
39. Campbell KP, MacLennan DH, Jorgensen AO (1983) Staining of the Ca^{2+}-binding proteins, calsequestrin, calmodulin, troponin C, and S-100, with the cationic carbocyanine dye ''Stains-all''. *J Biol Chem* 258:11267–11273.
40. Zacharius RM, Zell TE, Morrison JH, Woodlock JJ (1969) Glycoprotein staining following electrophoresis on acrylamide gels. *Anal Biochem* 30:148-152.
41. Rosenfeld J, Capdevielle J, Guillemot JC, Ferrara P (1992) In-gel digestion of proteins for internal sequence analysis after one- or two-dimensional gel electrophoresis. *Anal Biochem* 203:173–179.
42. Shechter A, Aflalo ED, Davis C, Sagi A (2005) Expression of the reproductive female-specific vitellogenin gene in endocrinologically induced male and intersex *Cherax quadricarinatus* crayfish. *Biol Reprod* 73:72–79.